Permeation Characteristics of Aqueous High Polymer Solutions

David F. James* and David G. Kimbell

Department of Mechanical Engineering, University of Toronto, Toronto, Canada M5S 1A4.
Received October 19, 1987

ABSTRACT: The permeabilities of concentrated aqueous solutions of partially hydrolyzed poly(acrylamide) (PAAm) and of poly(ethylene oxide) (PEO) were measured by sedimentation. The PAAm was tested in deionized water and in solutions of NaCl to determine the effect of ionic strength on solution permeability. For PAAm without NaCl, the permeability data indicate that the entangled chains behave hydrodynamically as a uniform fibrous porous medium. When NaCl was added, the permeability increased and, for sufficient salt, the results were consistent with predictions based on the blob concept and scaling laws. As for PEO, the permeability data for this neutral polymer also follow scaling laws. The permeability of these solutions was also measured by a technique in which a solution was confined in a cell with semipermeable walls and the pressure drop across the cell was measured for low flow rates of solvent through the cell. This technique provided reproducible results only for PAAm in deionized water but the measured permeability differed significantly from that obtained by sedimentation.

Introduction

The permeability of a concentrated polymer solution is a relevant parameter when there is relative motion between the solvent and polymer chains. In these situations, the rate of flow through the entangled polymer chains, or "skein", is dictated by the hydrodynamic resistance of the chains. This resistance is usually expressed by the inverse property, the permeability k, as defined by Darcy's law for porous media. One instance when this property is relevant is when macromolecules are adsorbed on surfaces over which there is flow; when the thickness of the adsorbed layer is a significant fraction of the width of the flow channel—as happens, for example, when water-soluble polymers bind to rock pores in enhanced oil recovery—the flow resistance of the adsorbed chains contributes to the flow resistance of the channel. Permeability is also relevant in processes such as flocculation and ultrafiltration. Hence it is important to establish the permeation characteristics of the polymers associated with these applications.

One such polymer is poly(acrylamide) (PAAm) because it is widely used in waste water treatment and in oil reservoir polymer flooding. Commercial PAAm, which is available as the sodium salt, is partially hydrolyzed (or is a copolymer of acrylamide and sodium acrylate). Because PAAm is a polyelectrolyte, configuration of the chains depends on the number of ions present in the solvent and hence ionic strength is expected to affect the permeability of PAAm in water.

The measurement of polymer skein permeability is generally done by sedimentation in an ultracentrifuge. In 1954, Ogston and Woods[1] made use of the idea that sedimentation of a concentrated polymer solution is equivalent to the flow of solvent through stationary polymer chains. More recently, Mijnlieff and Jaspers[2] used Darcy's law in combination with irreversible thermodynamics to establish a simple relation between the sedimentation coefficient S of a concentrated solution and the permeability k:

$$k = \frac{\eta_1 S}{C_2(1 - \bar{v}_2\rho_1)} \tag{1}$$

where η is viscosity, C is concentration, $\bar{v}$ is partial specific volume, ρ is density, and the subscripts 1 and 2 denote solvent and polymer, respectively. This equation and sedimentation data have been used to find k for a wide variety of polymer/solvent systems.

In 1977, Brochard and de Gennes[3] predicted the permeability of a skein of long, flexible, linear polymer chains. They assumed that the skein exists as a network of "blobs" or minicoils and solvent flows through the space between the blobs. From scaling laws, the permeability of a polymer skein was predicted to vary with concentration according to the relation $k \propto C^b$, where b is −1.5 for good solvents and −2.0 for Θ-solvents. The majority of sedimentation tests of concentrated solutions of linear, flexible polymers have followed the scaling laws. Roots and Nystrom[4] compiled the results of all such sedimentation studies prior to 1978 and found that most of them yielded values of b between −1.3 and −2.0; the few that did not were explainable.

Most of the data collected by Roots and Nystrom were for polymers in organic solvents, and for these b was generally in the range −1.6 to −2.0. For the water-soluble polymers, b was between −1.3 and −1.7, except for Ficoll which had a value of −2.2. Additional permeability data for water-soluble polymers are found to be in the same range. Two samples of poly(ethylene oxide) (PEO) with molecular weights of order 10^5 have been tested,[5,6] and the data yielded $b = -1.6$. Two polyelectrolytes, hyaluronic acid and PAAM, were dissolved in salt or buffer solutions, and b values were −1.5 and −1.7 respectively.[7,8] The only other polyelectrolyte for which there are data is sodium polystyrene sulfonate (NaPSS).[9] The sedimentation velocity data for NaPSS in the absence of added salt are such that a value of b cannot be assigned to the data. Hence, available results indicate that scaling laws generally apply to water-soluble polymers but it is not yet clear if the application extends to polyelectrolytes in salt-free solvents.

An entirely different technique for measuring the permeability of concentrated polymer solutions has been developed by Jackson and James.[10] They attempted to measure the permeability of hyaluronic acid solutions by enclosing a solution between two microporous membranes, pushing solvent through it, and measuring the flow rate and pressure drop. Darcy's law was used to calculate k directly. The advantages of this technique over sedimentation are its simplicity and low cost relative to ultracentrifugation. This permeation cell technique produced a value of b of −1.0 for the hyaluronic acid. Ethier,[7] however, has pointed out that this is in direct contradiction to the results of several sedimentation studies of hyaluronic acid, all of which found b to be −1.5. He suggested that the discrepancy was caused by compaction of the hyaluronic acid chains in the permeation cell. Hence it has not been estabished if the permeation cell is a valid technique for the measurement of permeability.

Another means of predicting polymer skein permeability

0024-9297/88/2221-2363$01.50/0

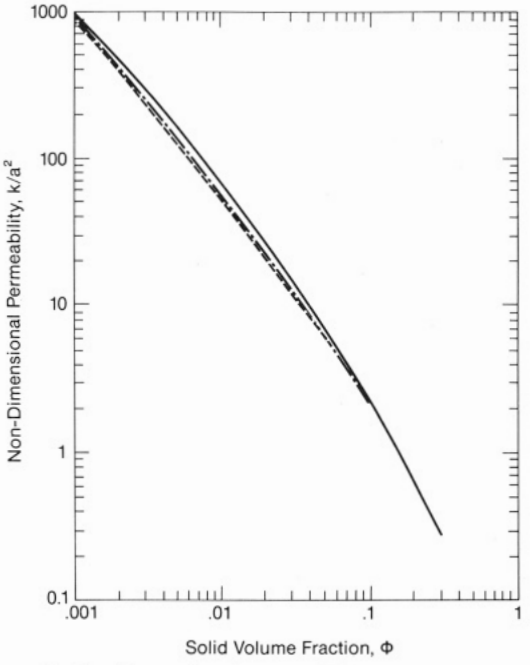

Figure 1. Nondimensional permeability, as a function of solid volume fraction, for three hydrodynamic models of uniform fibrous porous media. The fibers are circular with radius a: (—) Spielman and Goren;[11] (- - -) Jackson and James;[10] (– – –) Chesneau.[12] A straight-line fit to these curves for $\phi < 0.1$ has the form $k/a^2 = B\phi^{-1.2}$.

is to use the hydrodynamic models of fibrous porous media. For such media, the permeability is expressed by

$$k/a^2 = g(\phi) \tag{2}$$

where a is the radius of the fibers, ϕ is the solid volume fraction of the medium, and g is an algebraic function which depends on fiber configuration. Three models[10-12] have been developed for three-dimensional media of uniformly distributed fibers; the fiber configurations of the three models are quite different but the permeabilities predicted by them are similar, as shown in Figure 1. For $\phi < 0.03$, each curve is well approximated by a straight line of the form

$$k/a^2 = B\phi^b \tag{3}$$

where $b = -1.2$ and B is between 0.25 and 0.33, depending on which model is chosen. This value for b indicates that the hydrodynamic models are distinctly different from the blob concept, a difference which is to be expected because the hydrodynamic models assume that the polymer chains are distributed uniformly and therefore the solvent flows uniformly through the chains. While the blob concept has met with good success in predicting the permeability of concentrated solutions of nonionic polymers, for polyelectrolytes the repulsive forces may be strong enough to cause the chains to distribute themselves evenly. Should this be the case, a hydrodynamic model based on uniformly distributed fibers would be more appropriate.

The primary aim of the present work was to determine the effect of ionic strength on the permeation behavior of a commercial partially hydrolyzed PAAm in aqueous solution and to ascertain whether PAAm permeability follows predictions from scaling laws or from the hydrodynamic models. To provide a comparison to the PAAm data, nonionic PEO in water was also studied. A second objective was to assess the validity of the permeation cell technique by testing concentrated PEO and PAAm solutions in the cell and comparing the results to those obtained by sedimentation.

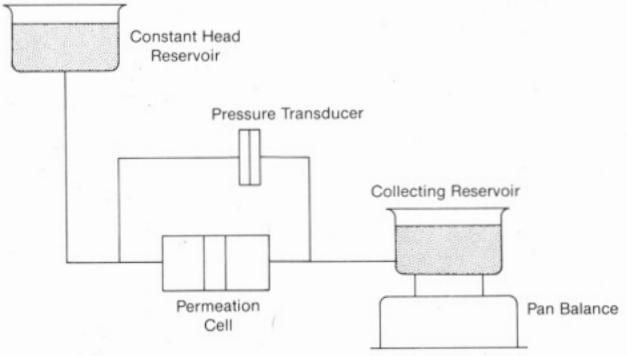

Figure 2. Apparatus for the measurement of permeability in the permeation flow cell.

Materials and Methods

Solution Preparation. In order to make the results from this study applicable to industrial situations, the polymers used in the study were commerical samples. The polymers were Separan AP273 (PAAm, $\bar{M}_w = 3.5 \times 10^6$, degree of hydrolysis 30%, from Dow Chemical), Polyox WSR-301 (PEO, $\bar{M}_w = 5.7 \times 10^6$, from Union Carbide), and SF-150 (PEO, $\bar{M}_w = 9.96 \times 10^5$, $\bar{M}_w/\bar{M}_n = 1.05$, from Toyo Soda). The molecular weights were determined by viscometric analysis using a Cannon-Fenske size 50 capillary viscometer (except for the SF-150 sample, which was characterized by the producer). Solutions were prepared by using dispersants, specifically, 1-propanol in the case of PEO and 2-propanol in the case of PAAm. The amount used was always 2% of the total solvent weight, the amount found by Kulicke et al.[13] to prevent aging of aqueous PAAm solutions. Both dispersants are also known to combat the growth of bacteria, which can cause polymer degradation. Further details of solution preparation may be found in ref 14.

Sedimentation Tests. PAAm solutions for the sedimentation tests were prepared in four different liquids: distilled (and deionized) water and 0.01, 0.1, and 0.5 M NaCl. The polymer concentration ranged from 1 to 10 kg/m^3, the lower limit being well above the critical concentration of 0.5 kg/m^3. The critical concentration, c^*, which separates the dilute from the semidilute regime, was estimated from $[\eta]c^* = 1$. The intrinsic viscosity $[\eta]$ was measured from viscometric tests of PAAm in 0.5 M NaCl. Solutions of PEO in distilled water were also prepared, the concentration range being 1–20 kg/m^3. The critical concentration c^* for this sample was estimated to be 0.5 kg/m^3, again using the inverse of the measured intrinsic viscosity. Thus the test solutions were sufficiently above the critical concentration to ensure overlap and, most likely, entanglement of the polymer chains.

A Beckman Spinco model E ultracentrifuge with a Schlieren optical system was used for all sedimentation analyses. Standard sedimentation procedure was followed and the temperature and rotor speed were 20 °C and 64 000 rpm for all tests. Photographs taken with the Schlieren system were very clear and each displayed a single sharp peak. At least six photographs were taken for each test. The distance r of the polymer skein boundary for the rotor axis was measured directly from each photograph. The data were plotted in the form of log r versus time, and the slope of a best-fit line through the data was used to calculate S. All data were quite linear, indicating radial dilution and hydrostatic pressure effects were negligible.

Permeation Cell Technique. The apparatus for the permeation cell technique is shown in Figure 2. The interior of the cell is a disk-shaped space, 37-mm diameter and 2.5 or 5.0 mm thick, in which a polymer solution is confined by semipermeable membranes. The membranes are 47-mm Millipore MF-type surface retention filters with pore sizes of 0.025 and 0.05 μm and each membrane is supported on each side by a thin stainless steel perforated plate having a solidity ratio of 25%. The cell is a simplified version of one used earlier[10] and further details are available in ref 14. The flow rate of solvent through the test cell was determined by weighing the efflux on an analytical pan

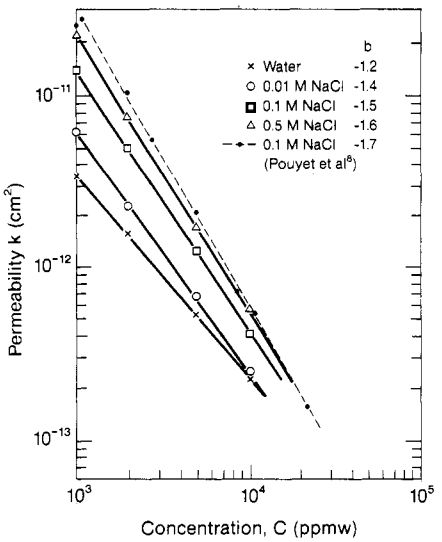

Figure 3. Permeability as a function of polymer concentration, for PAAm in water of different ionic strengths.

balance. The pressure drop across the cell was measured with a calibrated diaphragm-type differential pressure transducer.

In a typical experiment, a polymer solution was placed in the flow cell and the flow rate was measured for pressure drops ranging from 0 to 7×10^3 Pa. This yielded the flow resistance of the polymer skein and the membranes together. The permeation cell was then emptied on polymer and tested with solvent to determine the flow resistance of the membranes alone. The difference between the two measured resistances yielded the flow resistance R of the polymer skein. The permeability k was then calculated from the following form of Darcy's law:

$$k = \eta_1 L/AR \tag{4}$$

where A is the cross-sectional area available to flow and L is the distance between the membranes. The fluids tested in this way were PEO solutions in distilled water and PAAm solutions in both distilled water and 0.5 M NaCl.

A number of precautions had to be taken to obtain reproducible results. The membranes were degassed before use and the water (distilled and deionized at source) was deaerated and filtered through 0.45-μm pore size Millipore MF filters. This latter procedure was necessary to eliminate membrane clogging due to particulate matter in the water. Nevertheless, some clogging occurred in every experiment and this was evidently due to polymer entering the membrane pores. In the case of PAAm, the effect of clogging proved to be negligible, never increasing the overall flow resistance by more than 10%. But for PEO, it was a major factor. The membranes' flow resistance was found to triple and sometimes quadrupole within a few hours of flow initiation and generally reached a maximum after a cell volume of solvent had passed through the cell. After 6 h, the overall flow resistance began to drop, signifying a gradual loss of polymer from the flow cell. Since a complete experiment generally required at least 15 h, permeability measurement of PEO skeins was not possible with the permeation cell. Hence the only means of determining k for the PEO solutions was by sedimentation.

Results and Discussion

Sedimentation Tests. The permeabilities calculated from the sedimentation coefficients measured for PAAm in each solvent are plotted against concentration in Figure 3. The values of $\bar{v}_2$ used to calculate k from eq 1 were from the Polymer Handbook:[15] $\bar{v}_2 = 0.769$ and 0.834 cm^3/g for PAAm and PEO, respectively, in water. The value for PAAm in 0.5 M NaCl was not available, and it was assumed to the same as that for PAAm in water. The prior data by Pouyet et al.[8] are included in the figure, as are the values of b for each set of results.

Our results for 0.1 M NaCl in Figure 3 do not agree with the results of Pouyet et al. The discrepancy is not large

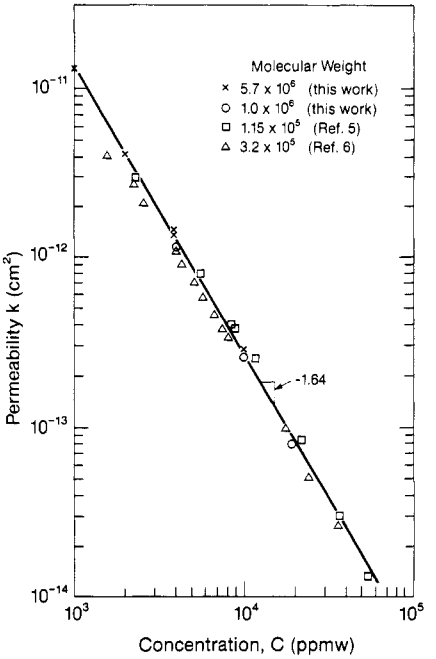

Figure 4. Permeability as a function of polymer concentration, for PEO in water.

and is comparable to the differences between investigators for PEO, as the next figure will show. It is thought that the discrepancy for PAAm is due to the degree of hydrolysis. Pouyet et al. stated the molecular weight (8.2×10^6) but not the degree of hydrolysis of their PAAm sample; while the former is not a relevant parameter, the latter can affect chain conformation and solvation and therefore the permeability of the solution.

Our data in Figure 3 clearly show that adding salt increases the permeability of a PAAm solution. Without salt, b is −1.2 which is the value for the hydrodynamic models, as given by eq 3. This agreement suggests that the polymer chains were evenly distributed and behaved hydrodynamically as a uniform fibrous porous medium. In this case, it is possible to estimate the effective hydrodynamic radius a of the chains. Rearranging eq 3, the expression for a becomes

$$a = (k\phi^{1.2}/B)^{0.5} \tag{5}$$

where $\phi = C\bar{v}_2$. When B is taken to be 0.28, then a is 5.3 Å. This corresponds to a diameter of 10.6 Å which is much larger than the physical cross-dimension of the chain. From known molecular bond angles, interatomic distances, and van der Waals atomic radii, the cross-dimension of a PAAm chain is found to be 4.6 Å at its widest point. The larger hydrodynamic diameter suggests that water molecules are packed around the PAAm chains in the absence of added ions. It should be noted, however, that this calculation of hydrodynamic diameter is based on models which assume that the solvent molecules behave as a continuum. While this is not an unreasonable assumption, the limits of continuum theorem are not really known and the figure of 10.6 Å must therefore be considered an estimate.

As salt is added to the PAAm solutions (Figure 3), the permeability increases and the slope of the data decreases. Adding salt evidently alters the conformation of the polymer chains such that they are no longer uniformly distributed. Conceivably, the added ions "shield" the chains so that they are able to approach each other. This would allow larger paths for flow between chains and would result in a lower flow resistance. At the highest ionic strength, $b = -1.6$, which is just below the value predicted

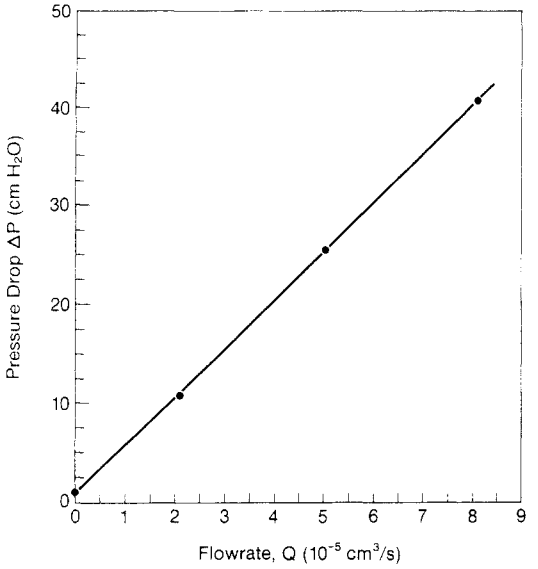

Figure 5. Typical plot of data from the permeation flow cell; confined solution was PAAm in water.

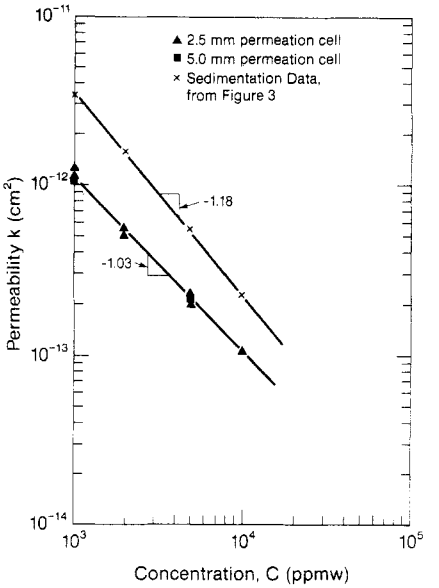

Figure 6. Comparison of permeability results for PAAm in water from ultracentrifugation and from the permeation cell.

by the scaling laws for polymers in good solvents. Hence as the ionic strength increases, the skein structure appears to change from a uniform distribution to a network of blobs.

Plotted in Figure 4 are the permeability measurements obtained by sedimentation of our PEO samples in distilled and deionized water. Also plotted are the results from two other sources for lower molecular weight PEO samples,[5,6] which agree well with our results. All of the results confirm that the permeability of a nondilute polymer solution is independent of the molecular weight of the polymer for sufficiently long chains. The slope of the data in Figure 5 is −1.6, well inside the range of values predicted by scaling laws. Thus while the polyelectrolytic PAAm appears to behave like a homogeneous fibrous porous medium in plain water, the nonionic polymer PEO appears to behave like a matrix of blobs.

Permeation Cell Tests. Shown in Figure 5 is a typical plot of ΔP versus flow rate Q for a permeation cell test with PAAm in distilled water, ΔP being the pressure drop for the polymer solution together with the membranes. The data for PAAm were always linear and hysteresis was never observed. The measured permeabilities were the same for the two membrane pore sizes tested (0.025 and 0.05 μm) and for the two distances between membranes (2.5 and 5.0 mm). There was no evidence of skein compaction, which seems to have occurred during the earlier permeation cell tests of hyaluronic acid. If compaction of the PAAm skeins had taken place, the pressure drop would not have been linear with flow rate until enough solvent had passed through the test cell, viz., enough to compress the chains. Since the flow volume for a series of concentrations was as low as 22% of the cell volume, and since the flow data were linear at all concentrations, polymer skein compaction did not likely occur in the permeation cell.

It is noted that the data in Figure 5 do not go through the origin. This zero-flow pressure drop was observed for most, but not all, flow cell tests of PAAm. It was an elusive phenomenon because it was not reproducible or even consistently positive or negative. It was also observed in tests of the membranes alone, after a test with polymer. This, and the fact that a small amount of membrane clogging occurred in every polymer tests, suggests that the phenomenon could have been due to polymer seeping into the membrane pores and creating different osmotic pressures across the two membranes. However, the effect was small, as Figure 6 indicates, and it did not affect the value of k, which was calculated by Darcy's law from the slope of the best-fit line through the ΔP versus Q data.

The permeabilities found from the permeation cell tests are plotted against concentration in Figure 6, along with permeabilities measured by sedimentation. The discrepancy between the two sets of results is significant. Clearly some major effect causes the permeation cell to produce significantly lower values of permeability. Compaction has already been ruled out but, had it occurred, the two lines would have intersected at some concentration, as Ethier[7] showed for hyaluronic acid. The possibility that the discrepancy was due to ultracentrifuge rotor speed was also investigated: tests of two solutions at two different rotor speeds indicated that S was independent of rotor speed, as expected. Since membranes are the fundamental difference between the permeation and sedimentation techniques, the most conceivable explanation for the discrepancy is that it was caused by an unknown but strong interaction between the polymer and membranes.

Some trial solutions of PAAm in 0.5 M NaCl were also tested in the permeation cell. Unfortunately, the data obtained were neither reproducible nor linear, suggesting that the polymer skein compacted during the tests. For this reason, permeation cell testing of PAAm in NaCl solutions was not completed.

Conclusions

Our permeability data for PEO and partially hydrolyzed PAAm solutions suggest—and suggest only—that water-soluble polymers follow scaling laws when the polymer is neutral, as in the case of PEO, or when the polymer is ionic and made neutral by sufficient ions in the solvent, as in the case of PAAm. For PAAm it was found that when the ionic strength is not sufficient, the permeability data deviate from scaling laws and, at extremely low ionic strength, the data follow predictions for a porous medium of uniformly distributed fibers.

Extensive tests with PEO and PAAm in the permeation cell show that this technique is not reliable for the measurement of polymer permeability.

Acknowledgment. The financial support of the National Science and Engineering Council of Canada is gratefully acknowledged. We are also grateful to Professor C. R. Ethier of this university for many helpful discussions.

Registry No. NaCl, 7647-14-5; Separan AP273, 37224-28-5; Polyox WSR, 25322-68-3.

References and Notes

(1) Ogston, A. G.; Woods, E. F. *Trans. Faraday Soc.* **1954**, *50*, 635.
(2) Mijnlieff, P. F., Jaspers, W. J. M. *Trans. Faraday Soc.* **1971**, *67*, 1837.
(3) Brochard, F.; de Gennes, P.-G. *Macromolecules* **1977**, *10*, 1157.
(4) Roots, J.; Nystrom, B. *Polymer* **1979**, *20*, 148.
(5) Roots, J.; Nystrom, B. *Chem. Scr.* **1980**, *15*, 165.
(6) Nystrom, B.; Boileau, S.; Hemery, P.; Roots, J. *Eur. Polym. J.* **1981**, *17*, 249.
(7) Ethier, C. R. *Biorheology* **1986**, *23*, 99.
(8) Pouyet, G.; Francois, J.; Dayantis, J.; Weill, G. *Macromolecules* **1980**, *13*, 176.
(9) Roots, J.; Nystrom, B. *Polymer* **1981**, *22*, 573.
(10) Jackson, G. W.; James, D. F. *Biorheology* **1982**, *19*, 317.
(11) Spielman, L.; Goren, S. L. *Environ. Sci. Technol.* **1963**, *2*, 279.
(12) Chesneau, C. P. M.A.Sc. Thesis, University of Toronto, 1985.
(13) Kulicke, W.-M.; Kniewske, R.; Klein, J. *Prog. Polym. Sci.* **1982**, *8*, 373.
(14) Kimbell, D. G. M.A.Sc. Thesis, University of Toronto, 1987.
(15) Brandrup, J.; Immergut, E. H. *Polymer Handbook*, 2nd ed.; Wiley: New York, 1975.

Morphology of Segmented Polybutadiene–Polyurethane Elastomers

Chi Li,† Steven L. Goodman,‡ Ralph M. Albrecht,‡ and Stuart L. Cooper*,†

Department of Chemical Engineering and Department of Veterinary Science, University of Wisconsin, Madison, Wisconsin 53706.

Received October 20, 1987

ABSTRACT: The morphology of segmented polybutadiene–polyurethanes containing a wide range of hard-segment content was studied with high-voltage electron microscopy (HVEM), high resolution scanning electron microscopy (SEM), and small-angle X-ray scattering. Specimens were prepared by thin film casting from solutions and by ultramicrotomy of bulk materials. Segmented polyurethanes with low hard-segment content have a morphology of dispersed, short, hard-segment cylinders embedded in a matrix of polybutadiene soft segments. An alternating hard- and soft-segment rodlike or lamellar microdomain structure was characteristic of materials with higher hard-segment contents. The length of lamellae or rods increased with increasing hard-segment content while the width of the lamellar or rodlike microdomains remained constant. At very high hard-segment contents, a morphology having a dispersed soft-segment phase was observable. It was also found that the shape of the dispersed soft-segment microdomains in the high hard-segment content samples was related to the details of sample preparation. The spacing between the hard- and soft-segment microdomains measured from micrographs was found to correlate well with the long spacing calculated from SAXS curves. In some cases the same sample was viewed by using HVEM and both secondary and backscattering electron imaging in the high-resolution SEM. The observation of similar morphologies with techniques based on such different imaging physics supports the contention that the structures are real and not a result of instrumental artifacts.

Introduction

The micromorphology of phase-separated polyurethane block copolymers and its influence on physical properties has been a focal point of much structure-property research.[1-7] Considerable attention has been devoted to characterization of the microdomains of the soft- and hard-segment phases since Cooper and Tobolsky postulated a phase-separated structure for segmented polyurethanes.[1] The first direct evidence for the formation of a two-phase structure was from the small-angle X-ray scattering (SAXS) studies by Bonart[8] and Clough et al.[9] SAXS profiles of polyether- and polyester-based polyurethanes show a prominent scattering peak at low angle, corresponding to a long spacing of about 10–25 nm.[10-13] This spacing was interpreted as being related to the interlamellar distance between microdomains.[11-13] On the basis of these observations, several models which describe the two-phase morphology have been proposed.[3,7,14,15] Since segmented polyurethanes possess a disordered two-phase morphology, detailed structural information on polyurethane morphology, however, cannot be derived from their single-peak X-ray scattering profiles without ambiguity.

Transmission electron microscopy (TEM) has been carried out on many polyurethane material systems. Both solvent casting and ultramicrotomy techniques have been employed to prepare thin films for TEM observation.[14,16-19] Ultramicrotomy can provide representative thin sections of the bulk morphology of the elastomer, but the low soft-segment glass transition temperature (T_g) requires cutting to be carried out with difficulty at very low temperatures. Thin films prepared by solvent casting techniques, on the other hand, may not represent the bulk morphology of the block copolymer since the process of phase separation depends upon the casting solvent and other conditions.[20] Lack of mass-thickness (atomic density) contrast between the hard- and soft-segment phases can cause imaging artifacts in the electron microscope as a result of poor focusing.[21,22] Osmium tetroxide has been used to selectively stain chemically unsaturated moieties in order to provide contrast between the hard- and soft-segment phases.[23] Recently, phosphotungstic acid (PTA) has been successfully applied to stain the amorphous region of polyamide materials.[24] An additional difficulty with electron microscopy of polyurethanes is that radiation damage and heating can cause the material to degrade. High-voltage electron microscopy (HVEM, a TEM at 1.0-MeV accelerating potential as compared to 100 keV in conventional TEM) reduces radiation damage to the polymer specimen due to decreased electron absorption.[25] This provides the opportunity for high-resolution electron microscopy. Additionally the ability to view selected areas of the sample at several angles of specimen tilt in the HVEM allows investigation of the sample's three-dimensional structure.[25]

Scanning electron microscopy (SEM) has been primarily used to investigate the surface topography of polymeric materials.[26] The bulk morphology of polymers can also

* Author to whom correspondence should be addressed.
† Department of Chemical Engineering.
‡ Department of Veterinary Science.

0024-9297/88/2221-2367$01.50/0